

# Photoacoustic tomography of vascular therapy in a preclinical mouse model of colorectal carcinoma

S.P. Johnson<sup>a</sup>, O. Ogunlade<sup>b</sup>, E. Zhang<sup>b</sup>, J. Laufer<sup>b\*</sup>, V. Rajkumar<sup>a</sup>, R. B. Pedley<sup>a</sup>, P. Beard<sup>b</sup>  
<sup>a</sup>UCL Cancer Institute, Paul O’Gorman building, University College London, 72 Huntley Street, London, UK, WC1E 6DD; <sup>b</sup>Dept. Medical Physics & Bioengineering, Malet Place Engineering building, University College London, Gower street, London, UK, WC1E 6BT;  
\* Currently at Julius Wolff Institute, Charité Universitätsmedizin, Augustenburger Platz 1, 13353 Berlin, Germany

## ABSTRACT

Vascular therapy in oncology exploits the differences between normal blood vessels and abnormal tumour neo-angiogenesis to selectively target cancer. For optimal treatment efficacy, and translation of novel compounds, the response of the tumour vasculature needs to be assessed. Photoacoustic tomography (PAT) is capable of this as it provides highly spatially resolved 3D images of vascular networks in biological tissue to cm depths. In preclinical models of cancer this is sufficient to encompass entire subcutaneous tumours, and can therefore be used to evaluate pharmacological intervention directed at the vasculature. In this study the vascular disrupting agent OXi4503 was used to treat subcutaneous tumour mouse models of two human colorectal carcinoma tumour types (SW1222, LS174T) at a range of concentrations (40mg/kg, 10mg/kg, 1mg/kg and sham dose control). The characteristic destruction of tumour vasculature caused by OXi4503 was observed by PAT and confirmed *ex vivo* via histology. Differences observed between the two tumour types assessed demonstrate the importance of tumour microenvironment and pathophysiology on response to therapy. Differential response to different doses of OXi4503 was observed, with outward tumour growth only seen once entire tumour viability had been re-established; this demonstrates the potential of PAT to act as a biomarker of response for the translation of novel anti-vascular compounds and also within the clinic. This study shows clearly that PAT can accurately assess the time course of drug action and relapse of pharmacodynamic effect in preclinical models of cancer and the important translational prospects for vascular targeted tumour therapies.

**Keywords:** Photoacoustic tomography; *in vivo*; vascular targeted therapy; tumour; biomarker

## 1. INTRODUCTION

In cancer research the attrition rate of compounds at the clinical stage following successful preclinical experiments has been estimated at a failure rate of 95% <sup>(1)</sup>. The low success rate of transition from novel compounds to clinically useful therapeutics highlights the importance of accurate preclinical models of disease and effective biomarkers for determining efficacy of treatment. An active area of research in oncology drug discovery programs is the field of vascular targeted therapies. Angiogenesis, the creation of new blood vessel structures from pre-existing vessels, is considered to be one of the fundamental hallmarks of cancer <sup>(2)</sup>, as it is required by all solid tumours to develop beyond  $\approx 1\text{mm}^3$  <sup>(3)</sup>.

The pathophysiology of solid tumour development is such that the vascular networks produced from aberrant neo-angiogenesis are an attractive target for therapeutic intervention. Two main categories of vascular targeted therapies have emerged, angiogenesis-inhibiting agents (AIAs) and vascular disrupting agents (VDAs). Whilst both work through different mechanisms, the former aiming to prevent further angiogenesis and tumour progression and the latter aiming to selectively destroy existing tumour vasculature, both require biomarkers of response that are inherently linked to the vascular state of the tumour.

Photoacoustic tomography (PAT) provides high spatially resolved visualization of tissue vascular networks <sup>(4)</sup>, and is therefore able to evaluate vascular abnormalities *in vivo* and provide biomarkers of response to vascular targeted therapies. Preliminary photoacoustic characterization of the LS174T and SW1222 subcutaneous colorectal mouse models, and the initial response to the VDA OXi4503, has already been reported <sup>(5)</sup>. This study demonstrated the ability of PAT to visualize the known characteristic destruction of the tumour central vasculature caused by OXi4503. The resultant central necrosis within 24 - 48hr was also shown, whilst leaving a viable rim of surviving tumour tissue at the periphery.

The current study expands on this work by using PAT to study the effect of OXi4503 action over a significantly longer time frame in both the SW1222 and LS174T subcutaneous mouse models. Different dose levels are also investigated in the SW1222 tumour line to attempt to demonstrate dose-response relationship.

## 2. Methods

### 2.1 Photoacoustic imaging system

The PAT system used (**Fig. 1**) has been described previously in the literature <sup>(6)</sup>. Briefly, the target area of interest was irradiated by a tunable fiber-coupled 50Hz Q-switched Nd:YAG pumped OPO excitation laser system with a beam diameter of 2cm. The deposition of optical energy within the tissue results in ultrasound waves that back propagate towards the planar Fabry-Perot polymer film interferometer (FPI) sensor (-3dB bandwidth of 39MHz). Measurement of the reflected light intensity of a continuous-wave interrogation laser scanned across the FPI enables changes in the optical thickness of the sensor, caused by the photoacoustic waves, to be mapped in 2D. Three-dimensional images were reconstructed from the detected photoacoustic signals using a time-reversal image reconstruction algorithm. This accounts for the frequency dependent acoustic attenuation exhibited by soft tissues via an acoustic equation of state which accounts for acoustic absorption <sup>(7)</sup>.

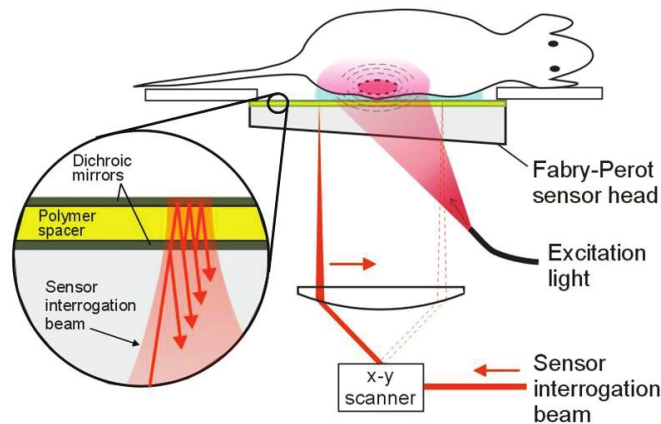


**Figure 1** Schematic of photoacoustic tomography system used with elements indicated

## 2.2 Xenograft model

All animal experiments were conducted in accordance with the guidelines for the welfare and use of animals in cancer research<sup>(8)</sup>. The human colorectal carcinoma cell lines SW1222 and LS174T were used as they are known to possess differing states of tumour vascularization in *in vivo* mouse preclinical models<sup>(9)</sup>. Tumour cell lines were kept and passaged in sterile tissue culture conditions (Incubator set to 37°C and 5% CO<sub>2</sub>, passaging within sterile class II downflow hood). For induction of tumours cells were prepared to a concentration of  $5 \times 10^7$  cells per ml and 100µl injected subcutaneously to female nude mice (CD1 nu/nu,  $5 \times 10^6$  total cells per injection). A total of n=6 LS174T and n=24 SW1222 mice were injected. Tumour development was monitored by caliper measurement, with the formula 'Length x width x depth x 6/π' used to calculate volume. Animals were used for PAI experiments when tumours were fully established.

## 2.3 *In vivo* PAT experiments

For *in vivo* imaging, animals were induced with 4% isoflurane anesthesia in O<sub>2</sub> and maintained at 1.5% isoflurane via face mask during PAT data acquisition. A drop of water was used to acoustically couple the FPI sensor and tissue region of interest and baseline datasets acquired. Animals were subsequently dosed i.v. via the tail vein with either a sham dose of saline (n=6 SW1222) or 40mg/kg (n=6 LS174T and n=6 SW1222), 10mg/kg (n=6 SW1222) or 1mg/kg (n=6 SW1222) OXi4503. Response to treatment was observed via follow-up PAT scans and caliper measurements. At 48 hours post-dose n=2 animals were terminated via a schedule 1 procedure and tumours excised for histological analysis to show evidence of central tumour necrosis. The remaining n=4 animals were monitored for vessel regrowth up to day 16 post-dose, at which point the animals were culled and tumours excised for histology.

## 3. Results

Histological analysis by Haematoxylin and Eosin staining showed basic tissue structure and morphology; **Figure 2** shows an example of n= 1 SW1222 tumour at 48 hours post either sham dose (panel A), 48 hours post 40mg/kg (panel B), or 16 days post 40mg/kg OXi4503 (panel C). A normally-distributed high cellular density is seen in both the sham control and day 16 samples (A and C), whilst non-cellular and cellular breakdown patterns can be observed in the 48 hour OXi4503 treated sample (B). The latter indicates that necrosis has taken place within the core of the OXi4503 treated sample, and is thus demonstrative of *in vivo* biological effect of treatment. The return to a normal high cellular density pattern at day 16 shows that the tumour has regained viability and that the action of OXi4503 has not been sustained beyond the initial pharmacodynamic response. This effect was noted in all treated tumours taken for determination of dosing efficacy.

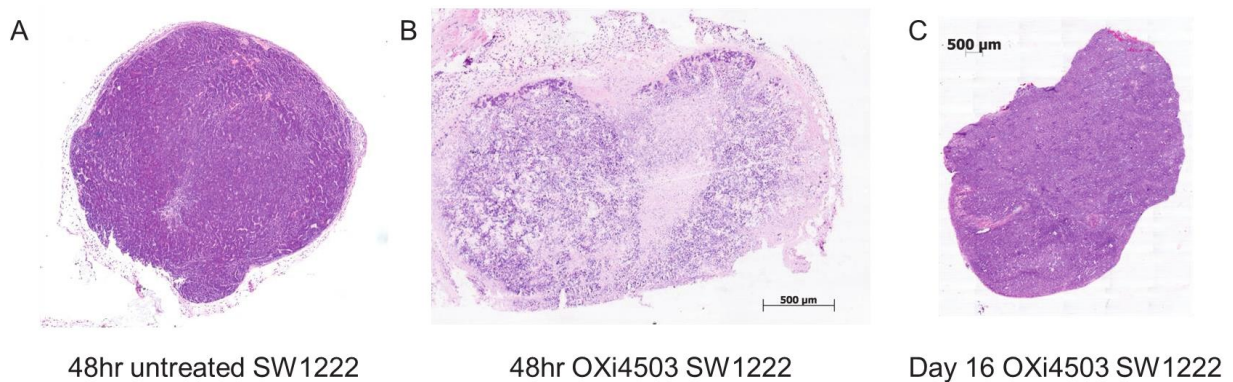


**Figure 2** Haematoxylin and Eosin staining of excised subcutaneous tumours

Results of the vessel regrowth experiment can be seen in the PAT data shown in **figure 3**. The n=1 SW1222 (top row) and LS174T tumour (bottom row) shown are representative of all tumours. The first column depicts pre-dose X-Y maximum intensity projections (MIP) over a depth range  $z=0\text{mm}-6\text{mm}$  of a tumour at baseline before dosing. The complete tumour capsule is located within this 6mm depth penetration. The tumour is visible in the central location of the PAT image in both SW1222 and LS174T images, with signal clearly visible from the centre of the viable tumour. Superficial skin blood vessels and tumour supplying blood vessels are also visible surrounding both these tumours. Post 40mg/kg of OXi4503 dose, seen here in the second column depicting 48 hours post-dose, avascular areas of necrosis, as evidenced by the lack of PAT signal (highlighted by red arrows) have developed within both SW1222 and LS174T tumours, whilst the image intensity from nearby non-tumour associated vasculature has remained constant; this effect is more pronounced in the SW1222 image. Images at 16 days after OXi4503 (third column) indicate that the central portion of the signal, where the tumour mass is sited, is almost entirely re-established within the SW1222 image and less so in the LS174T image, where avascular regions remain. Timepoints taken between 48hrs and 16 days (data not shown) show that the regrowth of signal occurs from the outside towards the centre of the tumour.

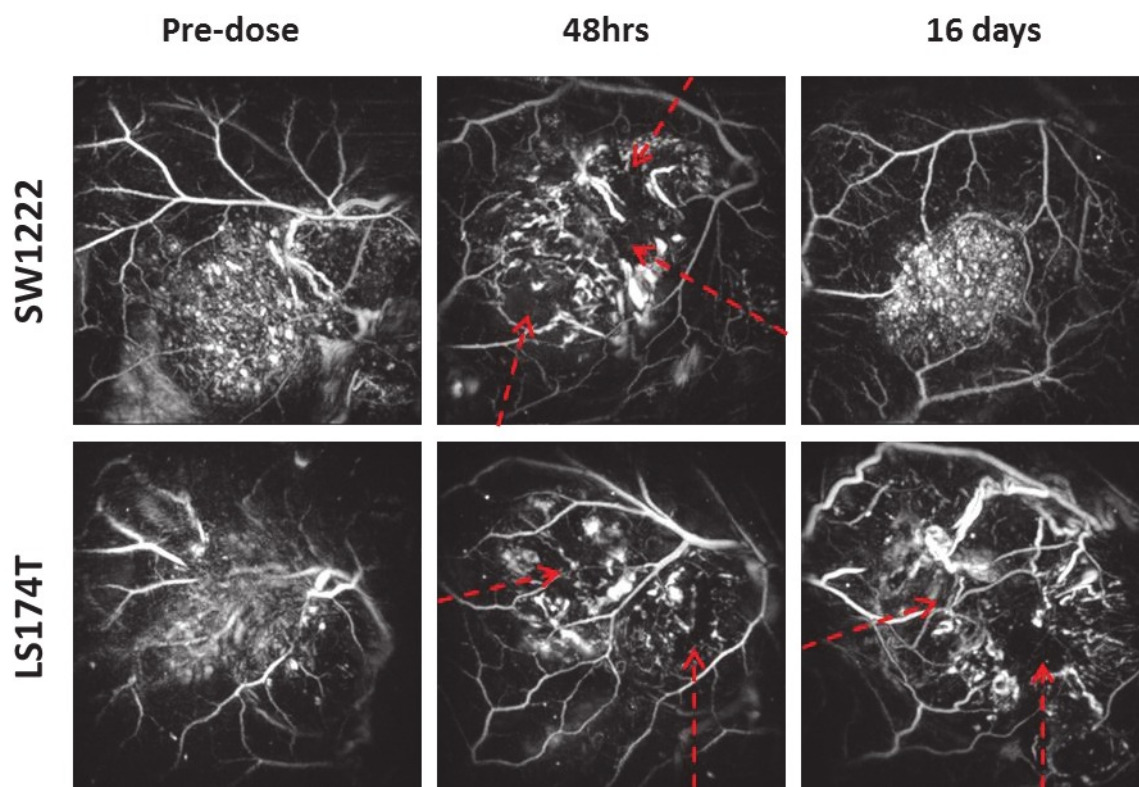


**Figure 3** Representative PAT images from n=1 SW1222 (top row) and LS174T (bottom row) subcutaneous tumour at baseline and 48hr and 16 days post 40mg/kg OXi4503 i.v. Images represent 14x14mm X-Y direction maximum intensity projections (MIP)

All animals were measured by calipers to determine tumour volume and track OXi4503 induced changes. The results for the drug titration experiment can be seen in **Figure 4**. Treatment with OXi4503 causes a dose dependent tumour growth delay with regard to volume, as can be seen in the graph presented in figure 4.

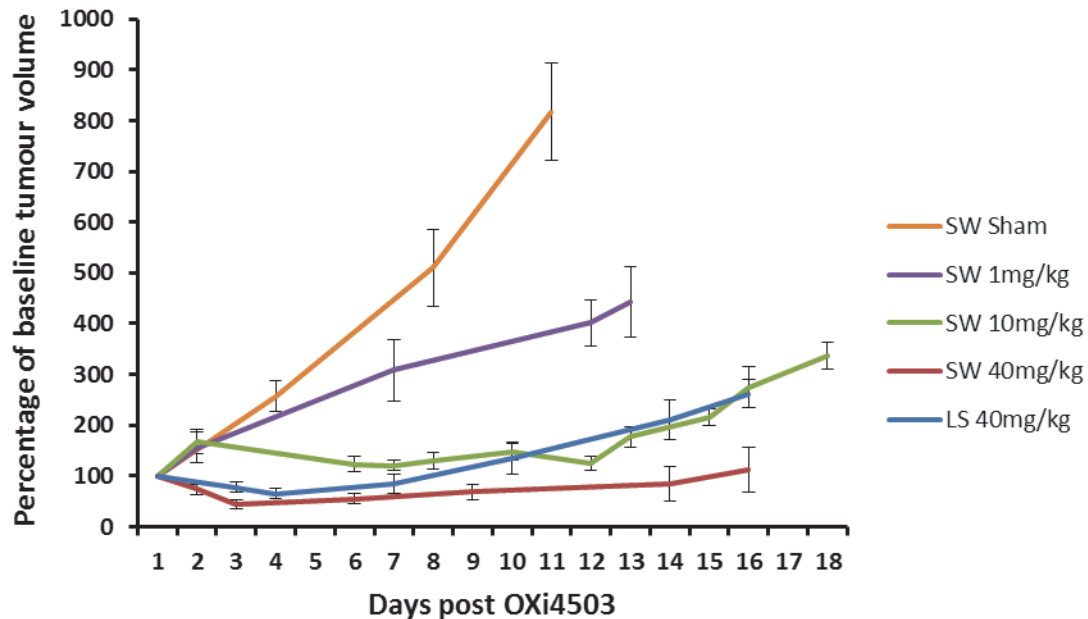


**Figure 4** volumetric assessment of subcutaneous tumours by caliper measurement

#### 4. Discussion

Vascular disrupting agents are known to cause central tumour necrosis through selective destruction of tumour blood vessels. The phenomenon of a surviving rim of viable tumour cells is well characterized by *ex vivo* histology, but has not previously been imaged *in vivo* in a non-invasive manner. As photoacoustic images haemoglobin are able to reveal vascular networks of the skin and tumour, they are ideally suited to monitor response to VDA treatment. This study shows that PAT signal from within the tumour internal vascular network can be detected, as can be seen in the pre-dose baseline images in figure 3. The subsequent loss of vascular network due to OXi4503 treatment is evident in our PAT images in figure 3, and shows that the treatment has been effective. This is reinforced by the histological data in figure 2 that shows onset of necrosis in the treated tumours. However, by day 16 the PAT signal has almost entirely returned within the SW1222 images, with the histological data also showing a return to typical structure. Images of LS174T tumours at day 16 show that some avascular areas remain (fig 3), presumably due to the heterogeneous nature of the vascular network within this type of tumour. PAT can therefore clearly follow the pharmacodynamic effect of OXi4503 vascular disruption within the tumour. Throughout this treatment period the normal vasculature remains unaffected, as is expected with VDA treatment, highlighting the tumour selective nature of OXi4503 action. The periphery of the tumour location in the PAT images would therefore relate to the known surviving viable rim of tumour cells. In this area PAT signal remains, indicating that the inward flow of blood to the tumour periphery is maintained. The re-growth of signal to re-supply the tumour with oxygen and nutrients originates from this surviving rim; this repopulation of vasculature is especially noticeable in the SW1222 images at day 16. The extent of pharmacodynamic action of OXi4503 can therefore be tracked *in vivo* non-invasively, which has clear benefits with regards to dosing schedules for patients and determining whether a specific dose has been effective. With this final point in mind it is interesting to note the response of the tumours to differing levels of drug treatment. Traditional caliper measurements are capable of differentiating between subsequent tumour growth delay at all dose levels and can provide a typical sigmoidal dose response relationship. Of interest is that PAT data can also show destruction of the central tumour blood vessels to varying degrees dependent upon dose. A

quantitative measure of variation of PAT signal may be possible from the data obtained, and would provide information instrumental to deciding drug efficacy in individual specific cases.

In summary we have shown clearly that PAT can assess the action of OXi4503 over time and inform when relapse of pharmacodynamic effect occurs. We have shown that this is possible in two clinically relevant preclinical models in a non-invasive, non-ionizing longitudinal manner, and that PAT can assess varying degrees of response caused by different drug administration concentrations. PAT therefore is a powerful tool that can provide invaluable information for the development of novel vascular targeted therapies in cancer research.

## 5. Acknowledgements

This work was carried out as part of King's College London and UCL Comprehensive Cancer Imaging Centre CR-UK & EPSRC, in association with the MRC and DoH (England). We would like to thank OXiGENE for kindly providing the VDA OXi4503 used in this experiment.

## REFERENCES

- [1] Kola I, Landis J. Can the pharmaceutical industry reduce attrition rates? *Nat Rev Drug Discov* 2004;3:711-5.
- [2] Hanahan D and Weinberg RA, "Hallmarks of cancer: the next generation", *Cell*. 2011 Mar 4;144(5):646-74
- [3] Judah Folkman, "What is the evidence that tumours are angiogenesis dependent?", *J Natl Can Inst* 1990 Jan 3;82(1):4-6
- [4] Beard, P. (2011). "Biomedical photoacoustic imaging", *Interface Focus*, 1(4), 602–631.
- [5] Laufer, J.; Johnson, P.; Zhang, E.; Treeby, B.; Cox, B.; Pedley, B.; Beard, P., "In vivo preclinical photoacoustic imaging of tumour vasculature development and therapy", *J Biomed Opt*. 2012 May;17(5):056016
- [6] Zhang E, Laufer J, Beard P, "Backward-mode multiwavelength photoacoustic scanner using a planar Fabry-Perot polymer film ultrasound sensor for high-resolution three-dimensional imaging of biological tissues", *Applied Optics* 2008 (47): 561-577.
- [7] Treeby BE, Zhang EZ, Cox BT, "Photoacoustic tomography in absorbing acoustic media using time reversal", *Inverse Problems* 2010, 26(11), 115003
- [8] Workman P, Aboagye EO, Balkwill F, *et al*, "Guidelines for the welfare and use of animals in cancer research", *British Journal of Cancer* 2010 (102):1555-1577
- [9] Emir EE, Qureshi U, Dearling JL, *et al*, "Predicting response to radioimmunotherapy from the tumour microenvironment of colorectal carcinomas", *Cancer Res* 2007 67(24):11896-905